



Assessing Close Range Photogrammetric Approach to Evaluate Pavement Surface Condition

Prof. Saad Issa Sarsam

Department of Civil Engineering
College of Engineering-University of Baghdad
E-mail:saadisarsam3@yahoo.com

Lect. Afrah Mekki Daham

Department of Surveying Engineering
College of Engineering-University of Baghdad
E-mail:afrah.daham@gmail.com

Assist. Lect. Amal Mahdi Ali

Department of Civil Engineering
College of Engineering-University of Baghdad
E-mail:amal.mahdi09@yahoo.com

ABSTRACT

The aim of this research is to adopt a close range photogrammetric approach to evaluate the pavement surface condition, and compare the results with visual measurements. This research is carried out on the road of Baghdad University campus in AL-Jaderiyah for evaluating the scaling, surface texture for Portland cement concrete and rutting, surface texture for asphalt concrete pavement. Eighty five stereo images of pavement distresses were captured perpendicular to the surface using a DSLR camera. Photogrammetric process was carried out by using ERDAS IMAGINE V.8.4. The results were modeled by using a relationship between the photogrammetric and visual techniques and selected the highest coefficient of determination (R^2). The first technique is efficient in evaluating the rutting with (R^2) range between (0.985-0.997), (R^2) for the scaling range between(0.990–0.999),as compared to the visual evaluation. The macrotexture of the asphalt concrete with a high (R^2) range between (0.982-0.999) and (R^2) for the cement concrete pavement surface texture range between (0.980 - 0.998), as compared to the sand patch method.

Keywords: evaluation, pavement, photogrammetry, surface texture, visual.

إستخدام إسلوب المسح التصويري ذي المدى القريب لتقييم حالة سطح الرصفة

الأستاذ سعد عيسى سرسم
قسم الهندسة المدنية
كلية الهندسة، جامعة بغداد

المدرس أفراح مكي دحام
قسم هندسة المساحة
كلية الهندسة، جامعة بغداد

المدرس المساعد أمال مهدي علي
قسم الهندسة المدنية
كلية الهندسة، جامعة بغداد

الخلاصة

الهدف من البحث اعتماد تقنية المسح التصويري ذي المدى القريب لتقييم حالة الرصفة السطحية ومقارنة نتائجه بما يعادلها من التقييم البصري. تم تنفيذ هذا التطبيق على شبكة الطرق في حرم جامعة بغداد في منطقة الجادرية لتقييم حالة سطح الرصفة الكونكريتية والرصفة الأسفلتية مثل (سمك نسجة السطح، تدهور السطح، التحدد). ثم التقاط خمسة وثمانين زوج من الصور المجسمة العمودية لأنواع مختلفة من فشاتل سطح الرصفة باستخدام كاميرا رقمية ، ثم أجريت عملية المعالجة بأستخدام برنامج ERDAS IMAGINE V.8.4 . إن مقارنة النتائج بين تقنية المسح التصويري وتقنية الفحص البصري كانت من ناحية الحساب الكمي للفشاتل و حساب شدة الضرر ثم نمذجتها بأستخدام أعلى قيمة لمعامل الترابط R^2 حيث إن تقنية المسح التصويري تعطي نتائج دقيقة لسطح الرصفة تتراوح أعلى قيمة لمعامل الترابط للتحدد R^2 ما بين (0.985 - 0.997). وما بين (0.990 - 0.999)



لتدهور الرصفة الكونكريتية مقارنة بطريقة الفحص البصري. اما بالنسبة لحالة نسجة سطح الرصفة الاسفلتية كانت R^2 تتراوح ما بين (0.982-0.999) ، ولنسجة سطح الرصفة الكونكريتية كانت R^2 (0.980-0.998) مقارنة بالطريقة التقليدية sand patch.

الكلمات الرئيسية: تقييم ، الرصفة ، المسح التصويري ، نسجة السطح ، البصري.

1. INTRODUCTION

Distress is defined as a condition of pavement structure that reduces the ability of a pavement to provide a safe and comfortable ride to its users. A variety of pavement distress can occur due to different causes such as loads, environmental problems, and poor pavement maintenance management, **NDOR, 2002**.

The evaluation of pavement surface condition is considered as a first step in scheduling the pavement maintenance program and assessment of budget requirements. Many techniques have been established for such process, such as GIS, video imaging with image processing software and even visual examination. Close-range photogrammetry may be used as a research tool in civil engineering such as pavement evaluation monitoring. ERDAS IMAGINE software enables surface conditions to be represented as ortho-image. Close-range digital photogrammetry is seen as a possible approach in providing geometrical imaging for pavement distress studies without physically touching the surface being measured. The results obtained by this technique are compared with visual inspection, **Chai, 2005**.

2. MANUAL DATA COLLECTION

One of the common methods of obtaining pavement distress information is by visual inspection. The alternative approach is surveying the roads in a vehicle traveling. Manual assessment can be finished directly on the road or later in the office, **Ahmed and Haas, 2009**.

2.1 Visual Observation

Visual observation of pavement distress is the most common method for monitoring pavement surface condition. This has been traditionally performed by trained engineers who walk along the road to assess the distresses and produce report sheets. This technique is more dangerous and time-consuming. In addition, the accuracy and consistency of the data also depend on the experience of the inspectors who perform the survey, **Oh, 1998**.

2.2 Stereo Photogrammetric System

Image-collection technology is the systems record pavement surface images using a video camera or photographic camera mounted on a survey vehicle, **Ali , 2013**.

Photogrammetric evaluation is either done manually by capturing image and specially designed workstations while trained crews rate the recorded road surface or automatically by computer image processing software, **ACSIRO, 2009**.

3. EXPERIMENTAL WORK

An attempt to investigate the potential capabilities and flexibility technique of the measurement-based vertical stereovision system and ERDAS IMAGINE 8.4 software in quantification of pavement distresses is being performed and comparison of this technique with the visual method will be adopted.



4. PHOTOGRAMMETRIC PROCESS

The work flow process for collection of stereo images for system photogrammetric using is made up of five steps:

1. The Frame Design.
2. Calibration of Camera.
3. Measurements of Ground Control Points
4. Image Data Acquisition.
5. Photogrammetric Processing (ERDAS IMAGINE Software V.8.4).

4.1 The Frame Design

This frame was designed by fixing the height of photo exposure is (1m.), the desired focal length is (24mm), photo overlapping (60%) therefore, the base line become (37.5cm.). As shown in **Fig.1**.

4.2 Calibration of Camera.

Photogrammetric technique is performed by using DSLR camera (Canon EOS 600D).The camera calibration was done by Photo Modeler Program. The report of calibration camera is shown in **Table 1**.

4.3 Image Capture Stage

Within the study area, Eighty five stereo pair images of pavement distresses were captured perpendicular to the surface using Cannon EOS 600D with a resolution of 18 mega-pixels). A single stereo image was captured with 60% overlap setting. As shown in **Fig.2**.

4.4 Measurements of Ground Control Points

Photogrammetric field work began with creation of certain distribution of control points around the area of distress. As shown in the **Fig.3**. At least 3GCPs spread across each image were marked and measured with a Total Station device (TOPCON, GTS 235). Part of the coordinates of ground control points are illustrated in **Table 2**. GCPs referenced by to the tow points which measured by using Differential Global Position system (TOPCON Hiper- GR3). As shown in **Fig.4**. Coordinates of Bench Mark points are listed in **Table 3**.

4.5 Photogrammetric Processing

This process was carried out using ERDAS IMAGINE software version 8.4.

4.5.1 Triangulation process

Triangulation is performed to estimate the (X, Y, and Z) locations of tie points in stereo model and exterior orientation parameters (EOP) of images can be computed. The distribution of the ground control points, and other points in the adjusted stereo model was shown in **Fig.5**. The adjusted (EOP) that resultant from triangulation process are listed in **Table 4**.

4.5.2 Creation ortho-images

After performing triangulation with ERDAS IMAGINE software, ortho-images were created. Window measurement tool in orthorectified image that necessary to measure lengths, area and other distress condition. Orthorectified image is shown in **Fig.6**.



5. VISUAL INSPECTION APPROACH

Distress approach of Visual techniques was based on **USDOT-FHA, 2003 and NDOR, 2002** which performed by walking along the roadways, visually assessing the distress areas. The equipments were used represented by tape measure, ruler graduated in millimeters. **Fig.7** shows the pavement distress measured by using tape measures.

6. MEASUREMENT of SURFACE TEXTURE

The average macrotexture depth of asphalt concrete and cement concrete pavement surface determined using “sand patch” method ASTM E 965. **Fig.8** shows the sand patch test setup.

7. THE RESULT AND DISCUSSION

Results were modeled by using a mathematical relationship between the two techniques and selected the highest coefficient of determination (R^2). Pavement distresses divided into asphalt concrete and cement concrete pavement distresses.

A. Asphalt Concrete of Pavement Surface

A.1 Rutting

Table 5 shows the assessment of rutting area, depth and intensity using (photogrammetric and visual methods).**Fig.9** shows the correlation of results obtained by using both methods, it shows high correlation as indicated by high coefficient of determination $R^2 = (0.997), (0.985), (0.996)$ for area, depth and intensity.

A.2 Macrotexture of asphalt concrete pavement

Table 6 shows the assessment of Macro texture area, depth and intensity using both testing methods (photogrammetric and sand patch MTD). **Fig.10** shows the correlation of results obtained by using both methods, it shows high correlation as indicated by high coefficient of determination $R^2 = (0.999), (0.982), (0.999)$ for area, depth and intensity respectively. Such result is agreed with the work **Alshareef, 2011, China and James, 2012**.

B. Cement Concrete Pavement

B.1 Scaling

Table 7 shows the assessment of scaling area, depth and scaling intensity using both testing methods. **Fig.11** shows the correlation of results obtained by using both methods, it shows high correlation as indicated by high coefficient of determination $R^2 = (0.999), (0.990), (0.998)$ for area, depth and intensity respectively.

B.2 Macrotexture of cement concrete pavement

Table 8 shows the assessment of Macrotexture area, depth and intensity using both testing methods (photogrammetric and sand patch MTD). **Fig.12** shows the correlation of results obtained by using both methods, it shows high correlation as indicated by high coefficient of determination $R^2 = (0.998), (0.980), (0.998)$ for area, depth and intensity respectively.



8. CONCLUSIONS

The following conclusions have been made:-

1. Photogrammetric technique provides the ability of accommodate more types of asphalt and concrete pavement surface distresses in the study area, especially, distress depth, and area by using a stereo vision technology.
2. Photogrammetric approach is efficient in evaluating the rutting with a high coefficient of determination ranged between (0.985 - 0.997) and the scaling with a high coefficient of determination ranged between (0.990 – 0.999), as compared to the traditional method of visual evaluation.
3. Photogrammetric approach is efficient in evaluating the macrotexture of the asphalt concrete with a high coefficient of determination ranged between (0.982 - 0.999) and cement concrete pavement surface with a high coefficient of determination ranged between (0.980 - 0.998), as compared to the traditional sand patch method.

REFERENCES

- ACSIRO, Australia's Commonwealth Scientific and Industrial Research Organization, 2009, *Automated detection of road cracks*, <http://www.csiro.au/solutions/psaa.html>.
- Ahmed, M. F. and Haas, C. T., 2009, *The Potential of Low Cost Close Range Photogrammetry towards Unified Automatic Pavement Distress Surveying*, Proceedings of the Annual Waterloo Demographic Center Conference.
- Ali, A. M., 2013, *Assessing Close Range Photogrammetric Approach to Evaluate Pavement Surface Condition*, M.Sc. Thesis, Department of Surveying Engineering, University of Baghdad, Baghdad, Iraq.
- Alshareef, H. N., 2011, *Assessing Asphalt and Concrete Surface Texture in the Field*, M.Sc. Thesis, Department of Civil Engineering, the University of Baghdad, Baghdad, Iraq.
- ASTM, American Society for Testing and Materials, 2006, *Road and Paving Materials*.
- Chai, L. T., 2005, *Evaluation of Cracks and Disintegration Using Close Range Digital Photogrammetry and Image Processing Technique*, M.Sc. Thesis, Department of Civil Engineering, College of Engineering, University technology Malaysia.
- China, S. and James, D., 2012, *Comparison of Laser Based and Sand Patch Measurements of Pavement Surface Macrotexture*, DOI: 10.1061/ (ASCE) TE.1943-5436.0000315, American Society of Civil Engineers.
- ERDAS, Inc., 2003, *IMAGINE OrthoBASE User's Guide*, ERDAS IMAGINE V8.4, Printed in Georgia.
- NDOR, Nebraska Department of Roads, 2002, *Pavement maintenance manual*.



- Oh, H., 1998, *Image Processing Technique in Automated Pavement Evaluation System*, University of Connecticut: Ph.D. Dissertation.
- USDOT-FHA , 2003, *Distress Identification Manual for the Long Term Pavement Performance Program*, FHWA-RD-03-031, US Department of transport.

NOMENCLATURE

R^2 : coefficient of determination.
 ω : rotation angle around the x axis.
 ϕ : rotation angle around the y axis.
 κ : rotation angle around the z axis.
DGPS: differential global position system
DSLR: digital single lenses reflex
Elev.: elevation
EOP: exterior orientation parameters
ERDAS: earth resources data analysis system
GCPs: ground control points
GIS: geographical information system
GR3: grade r3

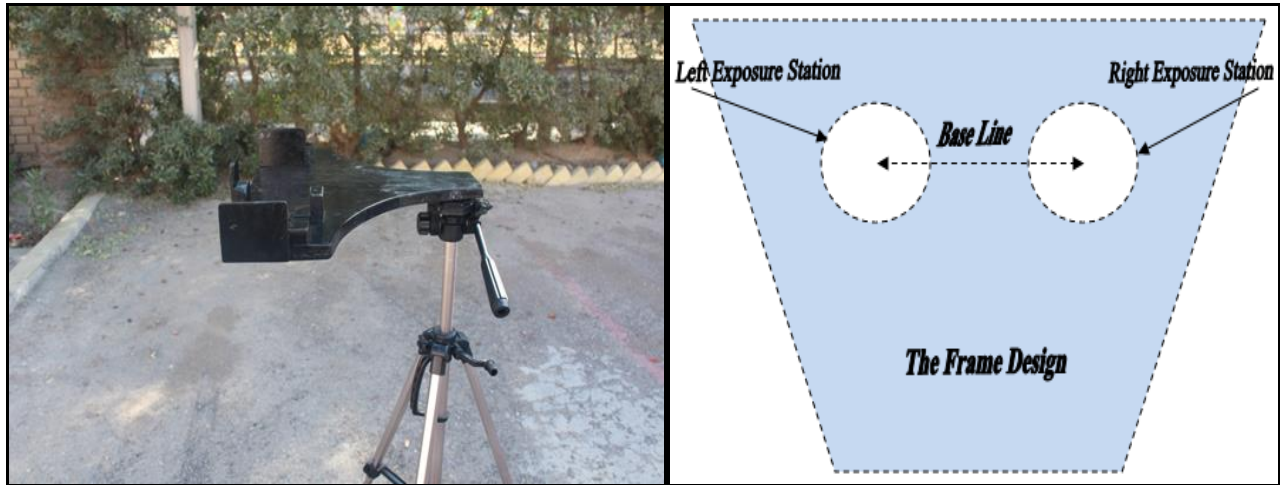


Figure 1. The designed frame and camera.

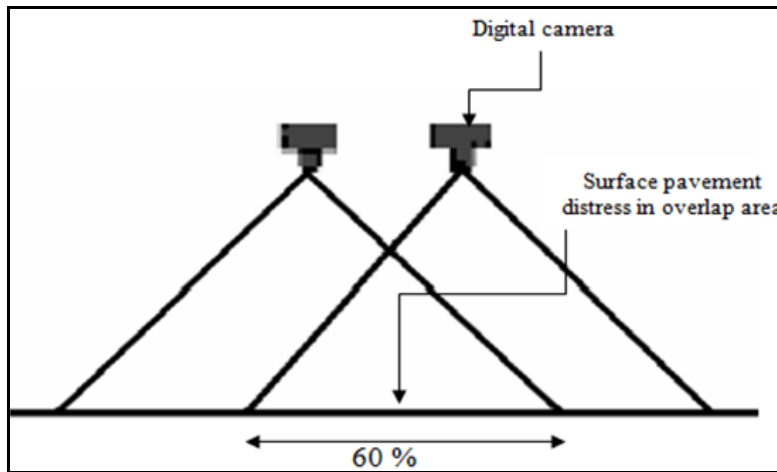


Figure 2. Stereo overlap image (60%).



Figure 3. Ground control point around distress area.



Figure 4. Sketch of two GPS points at the study area and DGPS device.

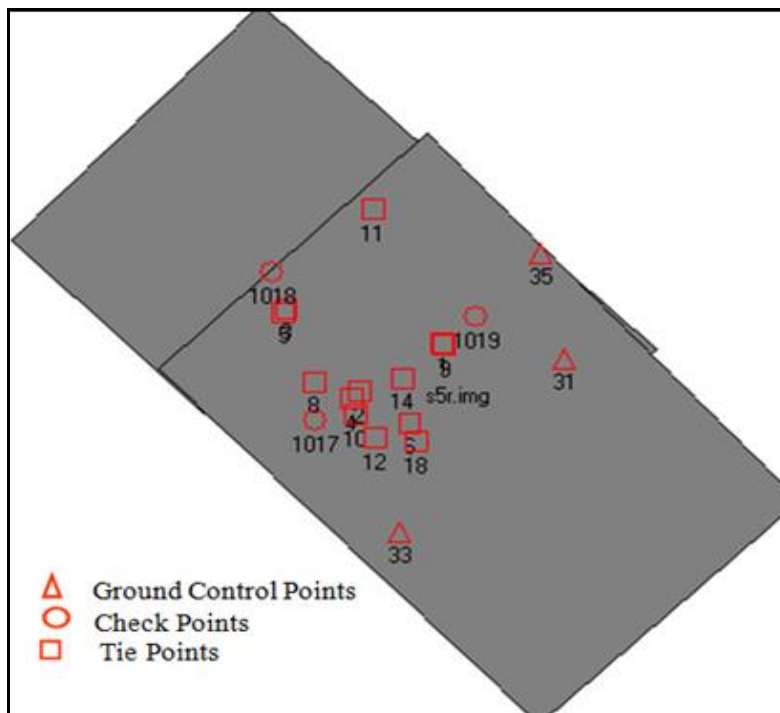


Figure 5. Distribution of ground control points, tie points and check points in the adjusted stereo model.

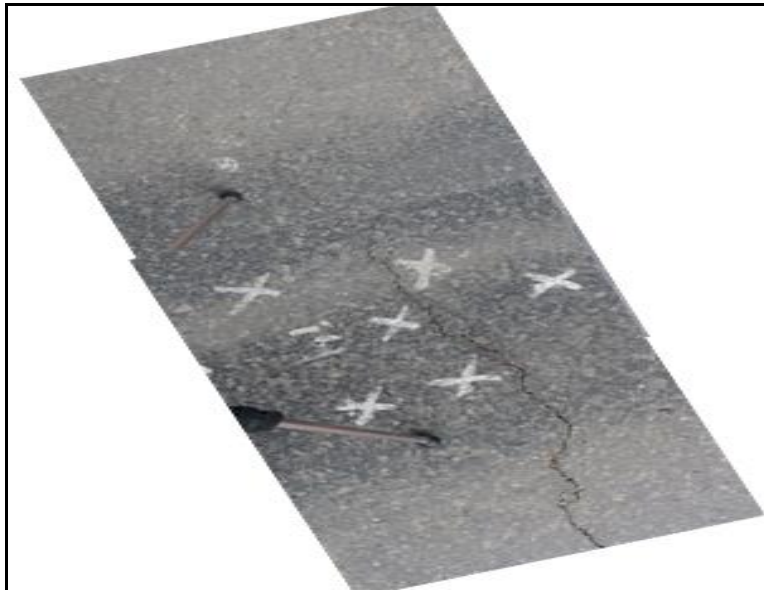


Figure 6. Orthorectified Image.

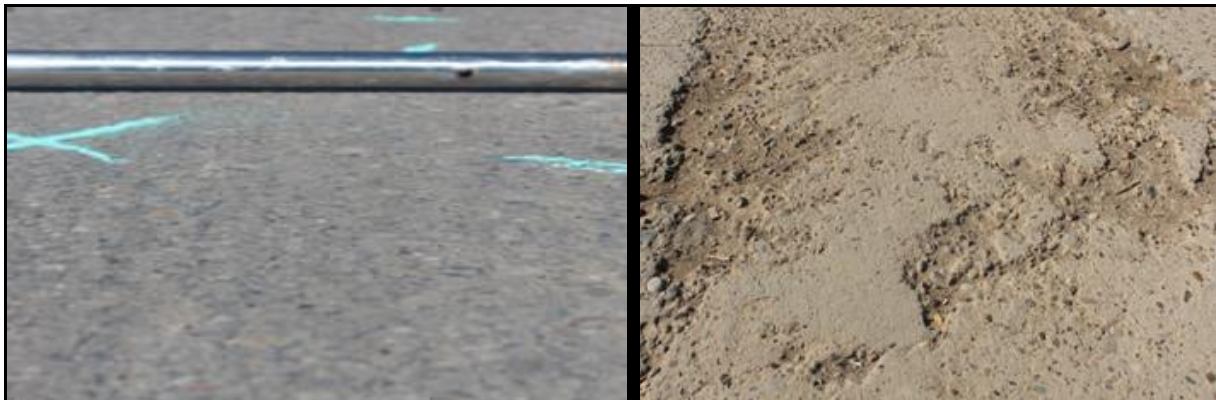
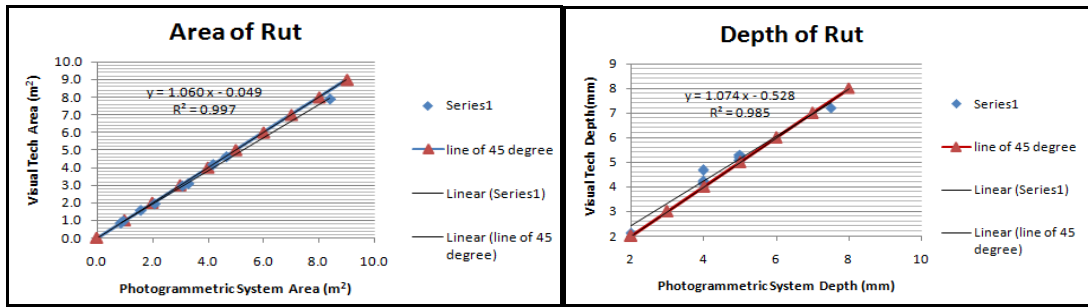


Figure 7. Visual inspection

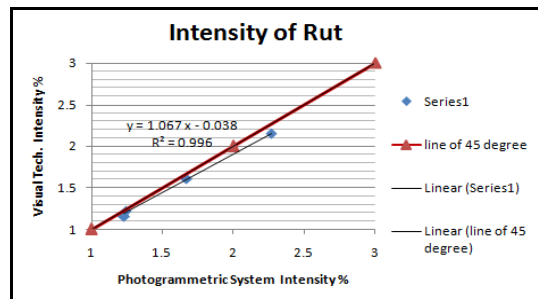


Figure 8. Sand patch test.



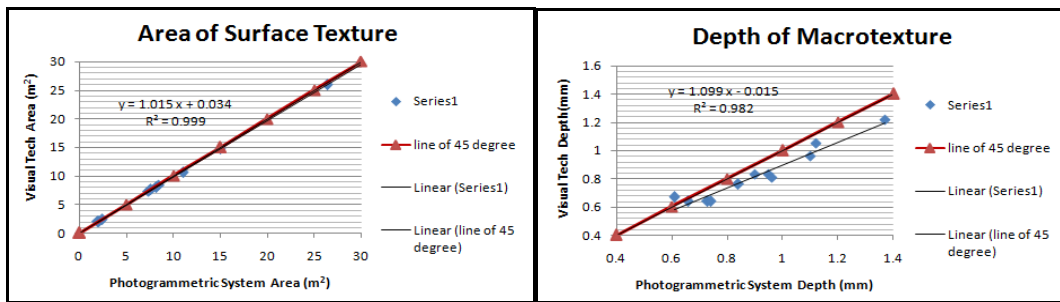
Correlation of photogrammetric rutting area with visual rutting area.

Correlation of photogrammetric rutting depth visual rutting depth.



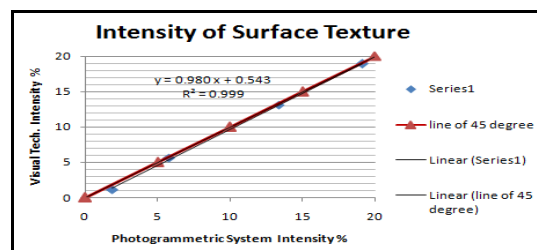
Correlation of photogrammetric rutting intensity with visual rutting intensity.

Figure 9. Correlation between two testing methods for evaluation of the rutting.



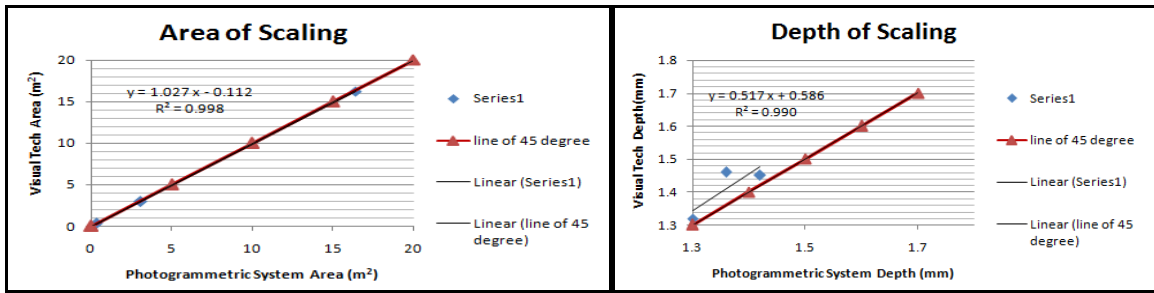
Correlation of photo. surface texture area with visual surface texture area.

Correlation of photo. macrottexture depth with visual macrottexture depth



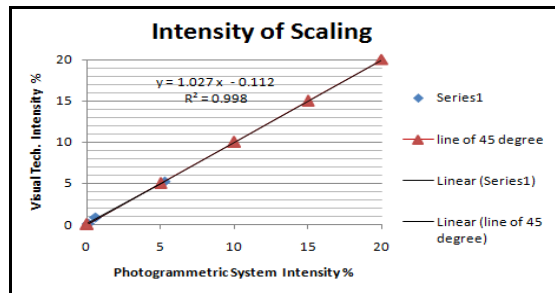
Correlation of photogrammetric surface texture area with visual surface texture area.

Figure10. Correlation between two testing methods for evaluation surface texture of asphalt concrete pavement.



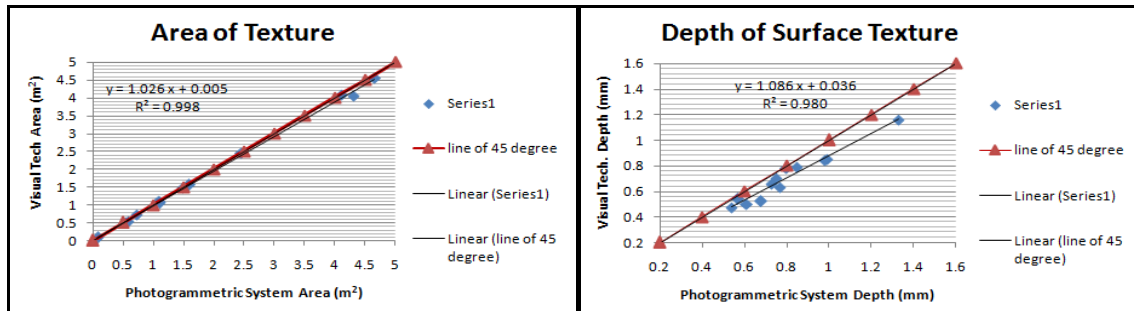
Correlation of photogrammetric scaling area with visual scaling area.

Correlation of photogrammetric scaling depth with visual scaling depth.



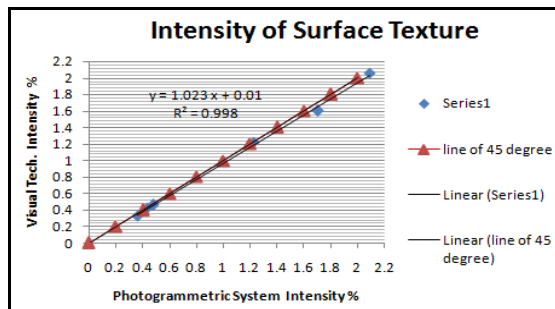
Correlation of photogrammetric scaling intensity with visual scaling intensity.

Figure 11. Correlation between two testing methods for evaluation of scaling.



Correlation of photogrammetric macrotecture with visual area macrotecture area.

Correlation of photogrammetric macrotecture depth with visual macrotecture depth.



Correlation of photogrammetric macrotecture area with visual macrotecture area.

Figure 12. Correlation between two testing methods for evaluation of macrotecture of cement concrete pavement.

**Table 1.** The calibration report, camera: Canon EOS 600D.

| Name | Value mm | Deviation (mm) |
|-------------------------------|---------------------------|-------------------------|
| focal length | 22.522933 | 0.008 |
| xp | 11.499973 | 0.005 |
| yp | 7.910362 | 0.005 |
| f h - format height | 15.113000 | 2.1×10^{-004} |
| f w - format width | 22.677364 | 2.2×10^{-004} |
| k1 - radial distortion 1 | -2.519×10^{-005} | 9.6×10^{-007} |
| k2 - radial distortion 2 | 4.488×10^{-008} | 1.7×10^{-008} |
| k3 - radial distortion 3 | $0.000 \times 10^{+000}$ | 0.00×10^{-000} |
| p1 - decentering distortion 1 | 2.094×10^{-005} | 9.4×10^{-007} |
| p2 - decentering distortion 2 | 1.125×10^{-004} | 8.0×10^{-007} |
| pixel size | 0.00470 | ————— |

Table 2. Part of coordinate ground control points coordinates.

| stereo pair ID. | point ID. | Northing(m) | Easting (m) | Elevation (m) |
|-----------------|-----------|-------------|-------------|---------------|
| 1 | 3 | 3682416.52 | 442628.099 | 33.746 |
| | 5 | 3682416.09 | 442627.967 | 33.756 |
| | 6 | 3682416.176 | 442628.118 | 33.748 |

Table 3. Coordinates of the two points measuring by DGPS system.

| point ID. | grid Northing (m) | grid Easting (m) | Elevation (m) |
|-----------|-------------------|------------------|---------------|
| point1 | 3682104.053 | 442365.913 | 34.037 |
| point2 | 3682314.976 | 442495.494 | 33.828 |

Table 4. Some of adjusted exterior orientation parameters.

| tie point ID. | Northing (m) | Easting (m) | Elev. (m) | omega(ω) | phi (ϕ) | kappa (κ) |
|---------------|--------------|-------------|-----------|-------------------|----------------|--------------------|
| 1 | 3682416.3421 | 442627.8161 | 34.7533 | 0.0442 | -0.8727 | -90.2681 |
| 2 | 3682416.4613 | 442628.2282 | 34.7491 | -1.0044 | 0.0343 | -87.8727 |



Table 5. Comparison result of rutting.

| sections | | no. of samples | sample ID. | area (m ²) | | depth (mm) | | intensity% | |
|----------------------|----------------|----------------|------------------|------------------------|---------------|--------------------|---------------|--------------------|---------------|
| section starting | section ending | | | visual inspection | photo. system | visual inspection | photo. system | visual inspection | photo. system |
| 1+250 | 1+300 | 1 | 33 | 4.20 | 4.16 | 2.0 | 2.14 | 1.24 | 1.22 |
| 1+300 | 1+350 | 2 | 34 | 3.31 | 3.08 | 4.0 | 4.12 | 1.23 | 1.16 |
| | | 3 | 38 | 0.88 | 0.85 | 4.0 | 4.17 | | |
| 2+150 | 2+200 | 4 | 57 | 3.10 | 2.95 | 5.0 | 5.29 | 1.67 | 1.61 |
| | | 5 | 59 | 1.60 | 1.57 | 5.0 | 5.09 | | |
| | | 6 | 60 | 0.97 | 0.96 | 4.0 | 4.26 | | |
| 2+250 | 2+300 | 7 | 64 | 4.68 | 4.60 | 5.0 | 5.20 | 2.27 | 2.15 |
| | | 8 | 65 | 2.10 | 1.94 | 7.5 | 7.20 | | |
| | | 9 | 67 | 8.40 | 7.86 | 4.0 | 4.67 | | |
| tested sample number | | 9 | regression model | y = 1.060x - 0.049 | | y = 1.074x - 0.528 | | y = 1.067x - 0.038 | |
| | | | R ² | 0.997 | | 0.985 | | 0.996 | |

Table 6. Comparison result of macrotexture of asphalt concrete pavement.

| sections | | number of samples | sample ID. | area (m ²) | | depth (mm) | | intensity% | |
|----------------------|----------------|-------------------|------------------|------------------------|---------------|--------------------|---------------|--------------------|---------------|
| section starting | section ending | | | visual inspection | photo. system | visual inspection | photo. system | visual inspection | photo. system |
| 0+450 | 0+500 | 1 | 17 | 8.47 | 8.39 | 0.73 | 0.64 | 5.81 | 5.65 |
| | | 2 | 18 | 11.05 | 10.58 | 0.90 | 0.83 | | |
| 0+700 | 0+750 | 3 | 25 | 15.00 | 14.69 | 0.84 | 0.76 | 13.35 | 13.10 |
| | | 4 | 26 | 26.40 | 25.92 | 1.10 | 0.96 | | |
| 1+300 | 1+350 | 5 | 78 | 2.04 | 1.97 | 0.95 | 0.83 | 1.88 | 1.15 |
| | | 6 | 32 | 1.98 | 1.97 | 0.74 | 0.64 | | |
| | | 7 | 39 | 2.38 | 2.34 | 0.96 | 0.81 | | |
| 2+150 | 2+200 | 8 | 56 | 42.00 | 41.39 | 1.37 | 1.22 | 19.17 | 18.90 |
| | | 9 | 57 | 8.16 | 7.97 | 1.12 | 1.05 | | |
| | | 10 | 59 | 7.40 | 7.32 | 0.61 | 0.67 | | |
| | | 11 | 60 | 7.64 | 7.57 | 0.66 | 0.64 | | |
| tested sample number | | 11 | regression model | y = 1.015x + 0.034 | | y = 1.099x + 0.015 | | y = 0.980x + 0.543 | |
| | | | R ² | 0.999 | | 0.982 | | 0.999 | |



Table 7. Comparison result of scaling of cement concrete pavement.

| sections | | number of samples | sample ID. | area (m ²) | | depth (mm) | | Intensity % | |
|----------------------|----------------|-------------------|------------------|------------------------|---------------|--------------------|---------------|--------------------|---------------|
| section starting | section ending | | | visual inspection | photo. system | visual inspection | photo. system | visual inspection | photo. system |
| 0+650 | 0+700 | 1 | 29 | 0.3280 | 0.3293 | 1.50 | 1.75 | 0.12 | 0.09 |
| 0+700 | 0+750 | 2 | 30 | 16.40 | 16.23 | 1.30 | 1.37 | 5.29 | 5.24 |
| 1+250 | 1+300 | 3 | 82 | 3.08 | 2.92 | 1.40 | 1.60 | 0.59 | 0.84 |
| tested sample number | | 3 | regression model | y = 1.007x + 0.063 | | y = 0.517x + 0.586 | | y = 1.027x - 0.112 | |
| | | | R ² | 0.999 | | 0.990 | | 0.998 | |

Table 8. Comparison result of surface texture of cement concrete pavement.

| sections | | number of samples | sample ID. | area (m ²) | | depth (mm) | | intensity% | |
|----------------------|----------------|-------------------|------------------|------------------------|---------------|--------------------|---------------|-------------------|---------------|
| section starting | section ending | | | visual inspection | photo. system | visual inspection | photo. system | visual inspection | photo. system |
| 0+300 | 0+350 | 1 | 6 | 0.59 | 0.53 | 0.99 | 0.85 | 1.6996 | 1.6001 |
| | | 2 | 11 | 0.09 | 0.08 | 0.75 | 0.70 | | |
| | | 3 | 12 | 4.31 | 4.05 | 0.80 | 0.78 | | |
| | | 4 | 14 | 0.73 | 0.72 | 0.77 | 0.63 | | |
| 0+350 | 0+400 | 5 | 31 | 1.100 | 1.096 | 0.54 | 0.47 | 0.36 | 0.33 |
| 0+450 | 0+500 | 6 | 16 | 4.11 | 4.09 | 1.33 | 1.16 | 1.224 | 1.218 |
| 1+350 | 1+400 | 7 | 40 | 4.66 | 4.55 | 0.68 | 0.52 | 2.09 | 2.06 |
| | | 8 | 41 | 2.46 | 2.44 | 0.61 | 0.50 | | |
| 1+400 | 1+450 | 9 | 46 | 1.49 | 1.47 | 0.85 | 0.79 | 0.433 | 0.425 |
| 2+200 | 2+250 | 10 | 61 | 1.11 | 1.05 | 0.73 | 0.66 | 0.48 | 0.46 |
| | | 11 | 62 | 0.54 | 0.50 | 0.98 | 0.84 | | |
| | | 12 | 63 | 1.60 | 1.56 | 0.57 | 0.54 | | |
| tested sample number | | 12 | regression model | y = 1.026x + 0.005 | | y = 1.086x + 0.036 | | y = 1.023x + 0.01 | |
| | | | R ² | 0.998 | | 0.980 | | 0.998 | |